Multi-scale model of solid oxide fuel cell: enabling microscopic solvers to predict physical features over a macroscopic domain

[Link to publication record in Manchester Research Explorer](#)

Citing this paper
Please note that where the full-text provided on Manchester Research Explorer is the Author Accepted Manuscript or Proof version this may differ from the final Published version. If citing, it is advised that you check and use the publisher's definitive version.

OPEN ACCESS

Multi-scale model of solid oxide fuel cell: enabling microscopic solvers to predict physical features over a macroscopic domain

Hamid Reza Abbasi,[a] Masoud Babaei,[a] Arash Rabbani,[b]

Constantinos Theodoropoulos,[a]

[a]*Department of Chemical Engineering, The University of Manchester, Manchester, M13 9PL, United Kingdom*
[b]*School of Computing, The University of Leeds, UK*
k.theodoropoulos@manchester.ac.uk

Abstract

In this study, a multi-scale model is developed to address the transport of gases, ions, and electrons inside a solid oxide fuel cell. Transport phenomena and electrochemical reactions inside the active layer of anode are simulated at the nanometer scale, while the rest of cell is simulated macroscopically at a coarser resolution. The microstructure of the anode side is reconstructed using pluri-gaussian random fields and the triple phase boundary (TBP), where all the electrochemical reactions are assumed to take place, is captured from the discretized (in voxels) image of the microstructure. Therefore, this multi-scale framework offers a much finer level of description for transport phenomena and for electrochemical reactions, significantly increasing the accuracy of numerical modelling of entire solid oxide fuel cells.

Keywords: Solid Oxide Fuel Cell, Multi-scale model, Triple phase boundary

1. Introduction

Fuel cells, as an alternative power generation device, have shown tremendous potential in clean, small- and large-scale electricity generation in recent decades. Fuel cells convert the chemical energy of a fuel (typically hydrogen) into electricity through electrochemical reactions. The energy conversion (chemical to electrical) is not limited by any thermodynamic law. Theoretically they can have 100% efficiency, whereas the efficiency of e.g., coal-powered stations is limited by the first and second law of thermodynamics and the maximum efficiency attainable is the Carnot efficiency. If hydrogen is to be utilized inside a cell as fuel, the only by-products of the electrochemical reactions would be oxygen gas and water.

Solid oxide fuel cells as the name suggests use a solid ceramic compound as the electrolyte to generate clean electricity (Singh, Zappa, and Comini 2021). SOFCs are well known for their high operating temperatures, which eliminate the need for metallic catalysts. Due to the convoluted interplay between different transport phenomena and chemical/ electrochemical reactions inside the cell, which span different length scales (Grew and Chiu 2012), complex models are needed to capture their behaviour. The electrode microstructure has a substantial effect on the overall electrochemical performance of the cell (dos Santos-Gómez et al. 2021). However, the size of an entire

fuel cell is far larger than the microscopic details of the electrodes to be considered in a macroscopic model. It is not, therefore, practically possible to numerically solve the mathematical equations governing the SOFC behaviour over an entire cell while maintaining a fine degree of description of microscopic details. This issue is thoroughly discussed by Grew and Chiu (Grew and Chiu 2012). Hence, most relevant works in the literature are focused either on macroscopic descriptions [4], component-level modelling [5], or on pore-scale modelling [6] of SOFC electrodes. These classes of models make multiple assumptions about the unresolved physics of the "other" scale. To bridge the gap between these two classes of numerical models, an integrated multi-scale numerical framework has been developed in this work by enabling a macroscopic model to obtain information directly from a pore-level model.

The macroscopic model uses the finite-element approach, and its domain covers the entire cell (fuel/air channels, electrolyte, and electrodes, and interconnects). In addition, a microscopic model is developed to simultaneously solve the coupled mass, ion, and electron transport equations, and chemical/electrochemical reactions in a three-dimensional microstructure of the SOFC electrode. Microscopic simulations are only performed on small segments (patches) of the microstructure. A "patch" [7] is a small spatial computational domain extracted from a larger volume/surface of interest, in order to facilitate the efficiency of complex computations. The contribution of this work is that the developed integrated, multi-scale model can resolve the physics linked to the fine microscopic topological features of the electrode microstructure over an entire length of an electrode in a particular fuel cell. This can improve the overall performance prediction of SOFCs, which is highly dependent on both their microscopic and macroscopic features.

2. Methodology

In this section, the two different models that are developed to address the multiscale problem are briefly discussed. The micro model solves the gas/electron/ion transport inside the active electrochemical layer. Using Fick's and Ohm's laws, mass/charge conservation equations can be written as follows. Knudsen diffusivity should also be considered due to small radius of pores. It can be approximated using kinetic theory of gases.

$$\nabla\left(-D_{H_2}\nabla c_{H_2}\right) = -\frac{\rho_{TPB}J}{2F}M_{H_2} \tag{1}$$

$$\nabla\left(-\sigma_{el}\nabla V_{el}\right) = -\rho_{TPB}J \tag{2}$$

$$\nabla\left(-\sigma_{io}\nabla V_{io}\right) = \rho_{TPB}J \tag{3}$$

Here, c_{H_2}, V_{el}, V_{io} are the hydrogen concentration, electronic potential, and ionic potential, respectively. ρ_{TPB} is the density of the triple phase boundary and J is charge transfer rate. This rate is only non-zero at the TPB. Therefore, all three governing equations (1-3) reduce to the Laplace equation anywhere else in the domain. For the microscopic model, these equations are solved over a representative volume element of a microscopic domain with regular hexahedral mesh. Each grid element represents a pixel in the tomographic image obtained from 3D imaging. Finite-volume method is employed to discretize equations in 3D space. Boundary conditions for micromodel consist of constant ion and electron potential at microstructure surfaces facing electrolyte and anode, respectively. Hydrogen concentration is also assumed constant at the boundary facing anode side. All other boundary conditions are zero-flux. Three coupled systems of linear equations resulting from discretizing equations 1-3 over the entire microscale domain are then solved until convergence using GMRES algorithm implemented in python.

The macroscopic model solves the mass and charge conservation equations inside an entire cell. The governing equations are the same as mentioned above. Since electrochemical reactions take place on the TPB in microscale, they cannot be resolved with the macroscale model. Instead, these reactions are modeled in the microscale model and then volume-averaged reaction rates are imported into macroscopic model as boundary conditions on the interfaces between electrolyte and porous electrodes. The charge transfer rate is assumed to follow the Butler-Volmer model.

$$J = J_0 \rho_{TPB} \left(\exp\left(\frac{2\beta F}{RT} \eta_{act}\right) - \exp\left(-\frac{2(1-\beta)F}{RT} \eta_{act}\right) \right) \qquad (4)$$

Where $J_0 \ [A/m]$ is the lineal exchange current density taken from data provided by Prokop et al. [8].

A schematic of the macroscopic and the microscopic model and their interactions is shown in Figure 1. The macroscopic domain contains fuel/air channels, porous electrodes, and electrolyte. The microscopic model, on the other hand, is limited to the active electrochemical site between the porous anode and the electrolyte. The microstructure is generated using pluri-gaussian random fields described in [9], and the location of TPB inside the microstructure is calculated with the algorithm discussed by Vivet et al. in [10].
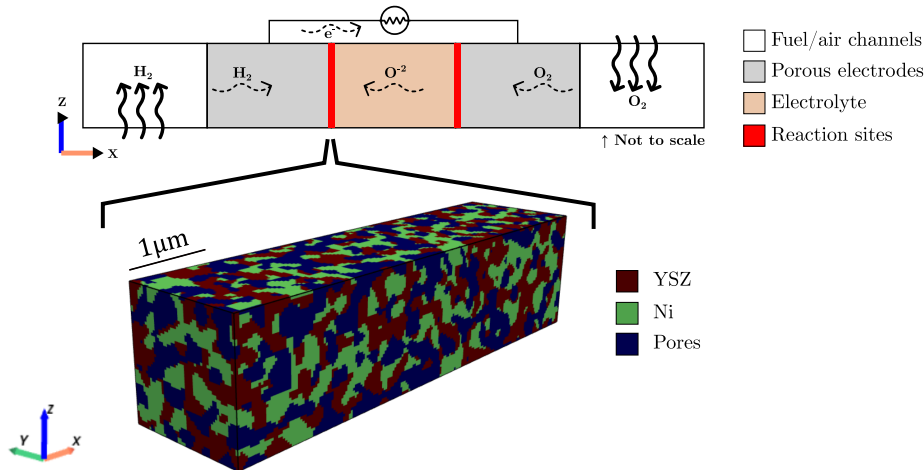
Figure 1 – *Schematic of the multi-scale numerical framework. The macroscopic model spans an entire cell, whereas the microscopic model only covers the electrochemical active layer between electrolyte and electrodes*

The transport equations are solved until convergence both in macro and in micro models. The information that is shared between two models are the physical features of the porous media (porosity, permeability), the effective current density exiting the electrolyte layer, operating voltage, and amount of overpotentials.

Geometrical parameters of the cell and physical properties of Nickel and YSZ are taken from papers by Tseronis et al. [4], and Shearing et al. (Shearing et al. 2010).

The numerical mesh that is used for the microstructure model is essentially the same as that of the voxelized image. Since the voxelized image is the finest description available of the real porous geometry, it has been decided that no smoothing should be performed on the reconstructed image. If the reconstructed geometry is to undergo smoothing, a finer numerical mesh can be constructed, which however would not be useful as its features would have been finer than the finest level of microstructure description available.

3. Results and discussion

In this section, the results of the multi-scale model combining the macro- and micro-scale models are presented and discussed. For the simulations, the operating temperature of the cell is assumed to be 900 °C. The density of the triple phase boundary is measured to be 9.456 μm^{-2}. The variation of the ion potential and current density in the microstructure electrochemical active layer of the anode side is shown in Figure 2. The YSZ phase inside the microstructure is on the left-hand side of the figure with the TPB lines depicted on the outer surface of the YSZ phase as black lines. On the right-hand side of the figure, the variation of the current density is shown on the TPB lines. To visualize the TPB lines, it was assumed that they have an artificial thickness of two pixels on each perpendicular direction. The top interface of the microstructure in this figure is adjacent to the electrolyte and the bottom side faces towards the porous anode layer. Due to the electrochemical reaction taking place on the TPB sites, the ion potential increases from the electrolyte interface (-0.341 V) to the porous anode interface (-0.5 V). The highest charge transfer rate is on the electrolyte interface, and it gradually reduces to zero as the distance from the electrolyte increases.

Changes in hydrogen concentration and electronic potential in the microstructure were insignificant, so they were not shown here. The micromodel is also capable of computing the local activation and concentration overpotential in the microstructure.
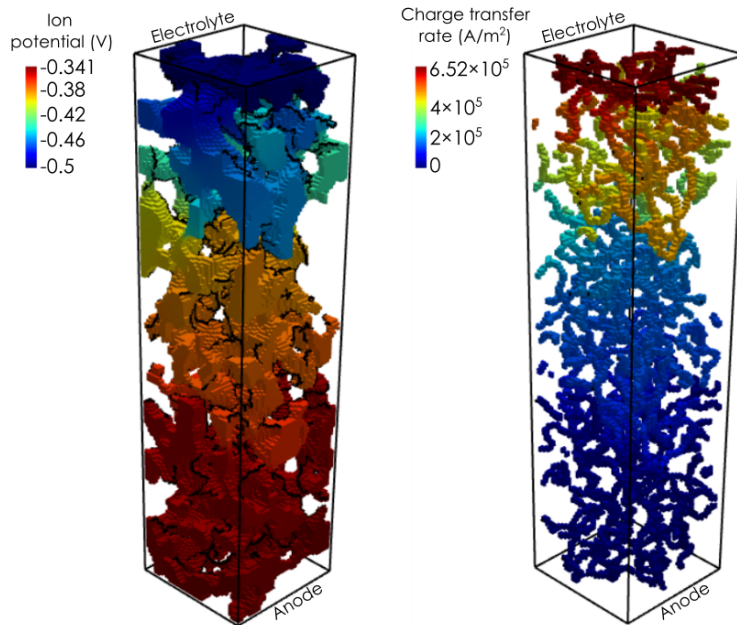

Figure 2 *– spatial variation of ionic potential and current density, respectively in the YSZ phase and on the TPB.*

Results of the multi-scale model are illustrated in Figure 3 below. Figure 3a depicts results from the macroscopic model, which the mass and charge transport through the entire cell, whereas Figure 3b depicts the results of the microscopic model. As mentioned above, the microscopic model solves the same transport equations as of the macroscopic model, with the exception that the micro-scale model also computes the electrochemical reactions on the TPB sites. As shown below, this enables the micro-scale model to capture the rate of

charge transfer locally with nanometer resolution. To demonstrate the capability of the multi-scale model, changes of ion potential and current density in the electrolyte and the porous anode are shown in figure 3a, whereas Figure 3b depicts the local variation of the same variables on the interface between electrolyte and porous anode, with much finer (nanoscale) resolution. For comparison, the size of each computational node in the macro-model is roughly 0.1 mm, whereas each computational node of the micro-model is only 25 nm. In Figure 3b, the minimum and maximum value, and the 95% confidence band of ion potential and current density in each slice of the microstructure in x direction (refer to Figure 1) is also shown.

The microscale model covers the electrochemical active layer only. Therefore, the rate of electrochemical reactions (or consequently current density, red curves in Figure 3) approaches zero when the distance from the electrolyte increases in the micromodel. The maximum current density on the electrolyte surface is then transferred to the macroscale model to simulate large-scale mass/charge transport. Potential difference across the micromodel (blue curves in Figure 3) implies the sum of activation and concentration overpotentials in the anode side. This potential difference is forced in the microscale model by macroscale simulation. As a result, until the mass and charge conservation criteria between the micro and macro domains are satisfied, there is an iterative loop between the micro and macro models. This link between micro and macro models allows macroscopic description of mass/charge transport inside a single cell while maintaining a microscopic resolution to explain electrochemical reactions at TPBs. It ultimately creates a framework to investigate the effects of microscopic features on macroscopic performance of the cell in our future studies.
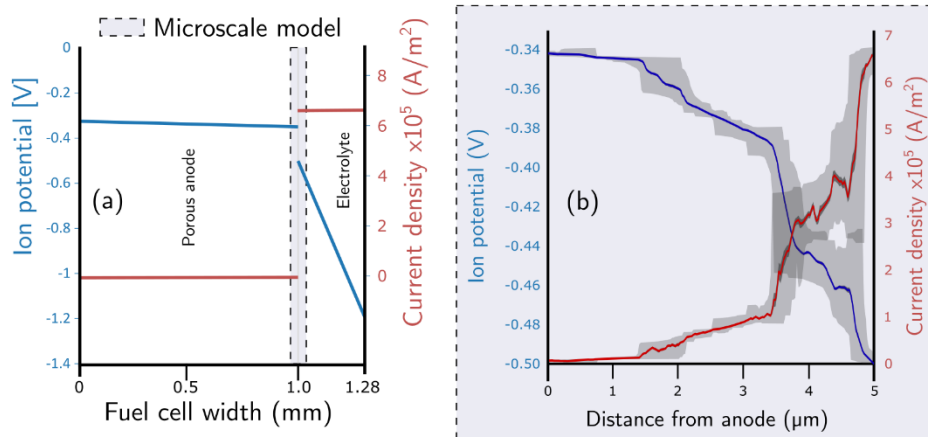
Figure 3 – *Variation of ion potential and current density across the width of the fuel cell both in macro- and micro-models with different numerical resolutions. (a) macroscale model. (b) microscale model*

4. Conclusions

A multi-scale numerical framework has been developed to study the mass/ion/electron transport inside the entire solid oxide fuel cell, from fuel channel to air channel with the capability of resolving the nanometer scale features inside the active electrochemical layer. This can help to achieve a more accurate description of electrochemical reactions taking place on the TPB and also on the double phase boundaries in the case of mixed ionic-electronic conductors, which ultimately increases the accuracy of the numerical model for predicting the performance of the entire cell or even an entire stack of cells.

The future research direction is to extend this multi-scale numerical framework to use multiple microstructures in parallel (patches) to capture the nanometric features and rate of electrochemical reactions across the length of the entire fuel cell, and even across multiple cells, significantly expanding the computational capabilities of the multi-scale model.

References

Bertei, A., V. Yufit, F. Tariq, and N.P. Brandon. 2018. 'A Novel Approach for the Quantification of Inhomogeneous 3D Current Distribution in Fuel Cell Electrodes'. *Journal of Power Sources* 396 (August): 246–56. https://doi.org/10.1016/j.jpowsour.2018.06.029.

Grew, Kyle N., and Wilson K.S. Chiu. 2012. 'A Review of Modeling and Simulation Techniques across the Length Scales for the Solid Oxide Fuel Cell'. *Journal of Power Sources* 199 (February): 1–13. https://doi.org/10.1016/j.jpowsour.2011.10.010.

Kevrekidis, Ioannis G, C William Gear, James M Hyman, Panagiotis G Kevrekidis, Olof Runborg, Constantinos Theodoropoulos, and others. 2003. 'Equation-Free, Coarse-Grained Multiscale Computation: Enabling Microscopic Simulators to Perform System-Level Analysis'. *Commun. Math. Sci* 1 (4): 715–62.

Moussaoui, H., J. Laurencin, Y. Gavet, G. Delette, M. Hubert, P. Cloetens, T. Le Bihan, and J. Debayle. 2018. 'Stochastic Geometrical Modeling of Solid Oxide Cells Electrodes Validated on 3D Reconstructions'. *Computational Materials Science* 143 (February): 262–76. https://doi.org/10.1016/j.commatsci.2017.11.015.

Prokop, Tomasz A, Janusz S Szmyd, and Grzegorz Brus. 2018. 'Developing Micro-Scale Heterogeneous Numerical Simulation of a Solid Oxide Fuel Cell Anode'. *Journal of Physics: Conference Series* 1101 (October): 012027. https://doi.org/10.1088/1742-6596/1101/1/012027.

Santos-Gómez, Lucía dos, Javier Zamudio-García, José M Porras-Vázquez, Enrique R Losilla, and David Marrero-López. 2021. 'Recent Progress in Nanostructured Electrodes for Solid Oxide Fuel Cells Deposited by Spray Pyrolysis'. *Journal of Power Sources* 507: 230277.

Shearing, P.R., Q. Cai, J.I. Golbert, V. Yufit, C.S. Adjiman, and N.P. Brandon. 2010. 'Microstructural Analysis of a Solid Oxide Fuel Cell Anode Using Focused Ion Beam Techniques Coupled with Electrochemical Simulation'. *Journal of Power Sources* 195 (15): 4804–10. https://doi.org/10.1016/j.jpowsour.2010.02.047.

Singh, Mandeep, Dario Zappa, and Elisabetta Comini. 2021. 'Solid Oxide Fuel Cell: Decade of Progress, Future Perspectives and Challenges'. *International Journal of Hydrogen Energy* 46 (54): 27643–74.

Tseronis, K., I. Bonis, I.K. Kookos, and C. Theodoropoulos. 2012. 'Parametric and Transient Analysis of Non-Isothermal, Planar Solid Oxide Fuel Cells'. *International Journal of Hydrogen Energy* 37 (1): 530–47. https://doi.org/10.1016/j.ijhydene.2011.09.062.

Tseronis, K., I.S. Fragkopoulos, I. Bonis, and C. Theodoropoulos. 2016. 'Detailed Multi-Dimensional Modeling of Direct Internal Reforming Solid Oxide Fuel Cells'. *Fuel Cells* 16 (3): 294–312. https://doi.org/10.1002/fuce.201500113.

Vivet, N., S. Chupin, E. Estrade, T. Piquero, P.L. Pommier, D. Rochais, and E. Bruneton. 2011. '3D Microstructural Characterization of a Solid Oxide Fuel Cell Anode Reconstructed by Focused Ion Beam Tomography'. *Journal of Power Sources* 196 (18): 7541–49. https://doi.org/10.1016/j.jpowsour.2011.03.060.